Near-Ultraviolet Magnetic Circular Dichroism Spectroscopy of Protein Conformational States: Correlation of Tryptophan Band Position and Intensity with Hemoglobin Allostery†

Deborah J. Vitale,‡ Robert A. Goldbeck,*,‡ Daniel B. Kim-Shapiro,‡,§ Raymond M. Esquerra,‡ Lawrence J. Parkhurst,|| and David S. Kliger‡

Department of Chemistry and Biochemistry, University of California, Santa Cruz, California 95064, and Department of Chemistry, University of Nebraska, Lincoln, Nebraska 68588-0304

Received December 9, 1999; Revised Manuscript Received March 15, 2000

ABSTRACT: The near-UV magnetic circular dichroism spectroscopy of the aromatic amino acid bands of hemoglobin was investigated as a potential probe of structural changes at the $\alpha_1\beta_2$ interface during the allosteric transition. Allosteric effectors were used to direct carp and chemically modified human hemoglobins into the R (relaxed) or T (tense) state in order to determine the heme-ligation-independent spectral characteristics of the quaternary states. The tryptophan magnetic circular dichroism (MCD) peak observed at 293 nm in the R state of *N*-ethylsuccinimide- (NES-) des-Arg-modified human hemoglobin (Hb) was shifted to a slightly longer wavelength in the T state, consistent with the shift expected for tryptophan acting as a proton donor in a T-state hydrogen bond. Moreover, the increase observed in the T-state MCD intensity of this band relative to the R-state intensity was consistent with the effect expected for proton donation by tryptophan on the basis of the Michl perimeter model of aromatic MCD. The peak-to-trough magnitude of the R − T MCD difference spectrum is equal to 30% of the total R-state peak intensity contributed by all six tryptophans present in the human tetramer; the relative magnitude specific to the two β37 tryptophans undergoing conformational change is estimated accordingly to be 3 times larger. The Trp-β37 spectral shift, about 200 cm^{-1}, is in good agreement with the shifts observed in other H-bonded proton donors and provides corroborating spectral evidence for the formation in solution of a T-state Trp β37−Asp α94 hydrogen bond observed in X-ray diffraction studies of deoxyHb crystals.

Although hemoglobin is perhaps the most extensively studied allosteric protein, the mechanism by which widely separated ligand binding sites cooperate to regulate oxygen affinity within the tetramer remains incompletely understood. The X-ray crystallographic structures of deoxyhemoglobin and oxyhemoglobin, first obtained by Perutz in the 1960s, established the structures of the two end states of hemoglobin allostery, the unligated tense (T)[1] and the ligated relaxed (R) states, respectively, with atomic resolution (*1*). Perutz et al. (*2*) later demonstrated that near-UV circular dichroism (CD) spectroscopy provided a convenient diagnostic tool for identifying the R and T quaternary states in solution. In a recent time-resolved application of this spectral diagnostic, nanosecond near-UV CD spectroscopy was used to follow the solution dynamics of the R → T transition in hemoglobin (*3*). That study revealed microsecond conformational changes at the aromatic $\alpha_1\beta_2$ interfacial residues preceding the relaxation at about 20 μs conventionally regarded as the R → T transition, implying that the allosteric transition proceeds through a compound kinetic mechanism involving at least two steps.

The present work examines the potential of magnetic circular dichroism (MCD) spectroscopy in the near-UV spectral region as a new tool for the study of allostery in human hemoglobin. The information obtained from such studies is expected to complement information from other spectral methods such as natural CD. Natural CD measurements tend to reflect global aspects of biomolecular structure because natural optical activity can be induced by chromophore−chromophore electronic interactions over distances as large as tens of angstroms within a biomolecule. In contrast, MCD is sensitive to aspects of molecular structure that directly affect the electronic structures of the magnetooptically active chromophores, such as heme and tryptophan, found in biomolecules. In this sense the information obtained tends to be more localized to a chromophoric site within a biomolecule.

The near-UV MCD of the aromatic amino acid tryptophan is found in the present work to offer a promising tool for monitoring the hemoglobin R → T transition. This promise arises from the fact that the transition between R and T quaternary structures entails large changes in local chain−chain interaction at the dimer−dimer interface (*2*). We investigated the extent to which these changes are reflected

† Supported by the National Institute of General Medical Sciences (NIH) Grant GM38549 and NSF Research Experiences for Undergraduates Grant CHE-9322464.

* To whom correspondence should be addressed.

‡ University of California.

§ Present address: Department of Physics, Wake Forest University, Winston-Salem, NC 27109-7507.

|| University of Nebraska.

[1] Abbreviations: T, tense state; R, relaxed state; CD, circular dichroism; MCD, magnetic circular dichroism; NES, *N*-ethylsuccinimide; IHP, inositol hexaphosphate.

10.1021/bi992823a CCC: $19.00
Published on Web 05/17/2000

in the near-UV MCD spectrum, in particular through their effect on the chemical environment of the tryptophan residue situated at the dimer−dimer interface, Trp β37. Tryptophan residues are of particular interest from the point of view of MCD spectroscopy because tryptophan generates the largest signals associated with the aromatic amino acids. Tryptophan is also unique in being the only amino acid with a positive MCD band at long wavelengths (*4, 5*), a feature that aids in the differential assignment of the aromatic MCD bands. Its MCD sign pattern is inverted from the pattern typically encountered in the other aromatic residues, the latter having a pattern corresponding to that expected from a simple electron-on-a-ring model (*6*).

Tryptophan's photophysical properties, particularly fluorescence, have been widely used as probes of intramolecular environment in proteins. In this regard, selectively probed fluorescence emission experiments have shown that Trp β37 contributes dominantly to the R − T fluorescence difference spectrum of human hemoglobin (*7*−*9*). The fluorescence properties of tryptophan were further exploited in a fluorescence-detected MCD study of tryptophan in cytochrome *c* by Sutherland and Low (*10*) that demonstrated the utility of that technique for MCD measurements in optically dense and biological materials. The sensitivity of the tryptophan chromophore's photophysical properties to protein environment is also apparent in the triplet-state lifetime, which lengthens to nearly a millisecond in human serum albumin (*11*). The absorption properties of tryptophan residues have also been measured, often by difference methods, as a probe of protein structural changes in response to perturbations in solvation (*12*).

Trp β37 is thus expected to be of particular spectroscopic interest as an MCD probe of the changing environment in the $\alpha_1\beta_2$ joint region of the interface during transitions in quaternary structure. The relaxed and tense conformations of the hemoglobin tetramer are stabilized by different sets of tertiary and quaternary interactions involving salt bridges and hydrogen bonds. In this regard, 17 pseudosymmetrically arrayed residues, including Trp β37, are involved in key interactions across the dimer−dimer interface. Hydrogen bonds connecting Trp β37 with Arg α92, Arg α141, and Pro α95 stabilize both the oxy and deoxy quaternary structures. An additional stabilizing interaction between Asp α94 and Trp β37, shown in Figure 1, is part of a network of salt bridges that stabilizes the T state (*13*). The low oxygen affinity of deoxyhemoglobin is attributed mainly to salt bridges that tether the C-terminal residues of both the α and β chains. The salt bridges of the α chain are made by the α carboxyl of Arg α141 to both the ϵ amino of Lys α127 and the α amino of Val α1. The guanidinium group of Arg α141 also interacts with the carboxyl group of Asp α126. In the β chain, the restraining salt bridges are made by the α carboxyl of His β146 with the ϵ-amino group of Lys α40 and by the imidazole of His β146 with the carboxyl group of Asp β94.

The constraints on the deoxyhemoglobin tense structure outlined above can be partially eased by chemical modification of the protein. In particular, a salt bridge between His β146 and Asp β94 can be perturbed by the irreversible modification of Cys β93 with *N*-ethylmaleimide to form *N*-ethylsuccinimide (NES) hemoglobin (*14*). [This is the only reactive sulfhydryl residue present in the native protein structure (*15*).] The bulky NES group prevents the formation of both the His β146−Asp β94 and His β146−Lys α40 salt bridges in deoxyhemoglobin (*16*). This repositions the C-terminal histidines but has little other effect on the protein structure (*17*). The NES modification both reduces the cooperativity of the tetramer (the Hill coefficient equals 1 at pH 7) (*16*) and increases the oxygen affinity of the β chains (*18*). Steric constraints created by the NES group keep the conformation of the proximal histidine near the oxy tertiary position (*14, 15*), shifting the equilibrium in favor of the higher affinity R state even in the absence of ligand (*17*).

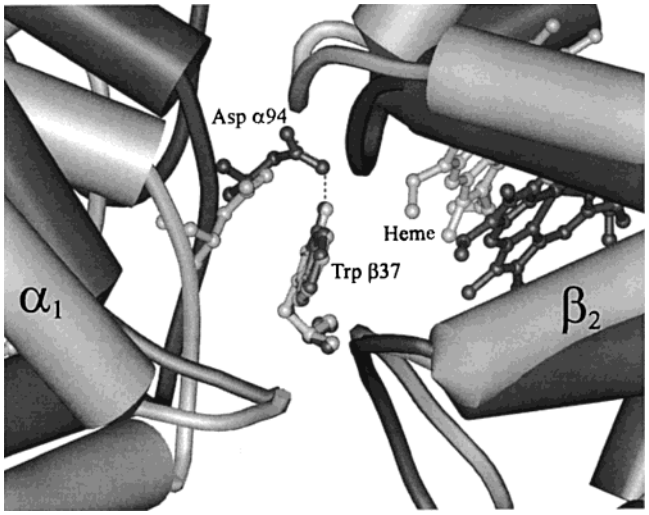

FIGURE 1: Diagram of the flexible joint region of the $\alpha_1\beta_2$ interface in human hemoglobin showing the interaction of Trp β37 with Asp α94. The R (light) and T (dark) crystallographic structures are shown overlapped and pivoted about Trp β37. The T-state hydrogen bond is indicated by the dotted line.

The removal of Arg α141 through digestion with carboxypeptidase B may also be used to modify hemoglobin (*16*). Like the NES modification, the des-Arg modification increases the oxygen affinity, in this case by roughly 15 times relative to that of human hemoglobin (*19*). Although there are no significant heme pocket perturbations in des-Arg-hemoglobin, increased mobility at the $\alpha_1\alpha_2$ interface and large changes in tertiary structure at both the amino and carboxy termini of the α chains result from the loss of interactions with Lys α127, Val α1, and Asp $\alpha_2$126 upon removal of Arg α141 (*19*).

The combined elimination of salt bridges via the NES and des-Arg modifications increases the ligand affinity and shifts the equilibrium further to the R conformation (*19*). NES-des-Arg-hemoglobin is thus characterized by a high oxygen affinity, loss of the Bohr effect, and noncooperative ligand binding. In the absence of the allosteric effector inositol hexaphosphate (IHP), it remains in the R conformation even when fully deoxygenated (R_0) (*1, 16*). The present work uses IHP to switch deoxy-NES-des-Arg-Hb from the R to the T state, permitting exploration of the near-UV MCD spectral properties of the quaternary states without interference from spectral effects arising from the heme ligation changes that would be required in native hemoglobin.

EXPERIMENTAL PROCEDURES

Fresh human hemoglobin was obtained in oxygenated form from a healthy donor by published procedures (*20*). Red

blood cells were washed in 1% NaCl solution, then centrifuged four times at 4000*g* prior to cell lysis with deionized water, and centrifuged again, at 10000*g*, after lysis. The supernatant was dialyzed overnight against 0.1 M sodium phosphate buffer. The hemolysate contained less than 5% Hb A_2 impurity, as determined by ion-exchange chromatography on a DE-52 matrix. The hemoglobin was concentrated and pelleted for storage by dropping small beads of concentrate into liquid nitrogen.

The NES modification to Cys β93 was based on published procedures (*15*). One gram of oxygenated human hemoglobin was brought to a concentration of 600 μM in heme in a 0.2 M sodium phosphate buffer at pH 7.15. *N*-Ethylmaleimide was added in a ratio of 5 mol/mol of hemoglobin. The reaction was carried out for 1 h at 25 °C and then stopped by 48 h of dialysis at 4 °C against 4 L of 0.016 M sodium phosphate buffer at pH 6.5, the buffer being changed four times. The NES modification was confirmed by optical absorption difference spectroscopy in conjunction with the Ellman's reagent test (*21*). Successful modification was indicated by an absorbance at 328 nm showing no protein sulfhydryl reaction with the Ellman's reagent. [Absorbance at 412 nm from reacted Ellman's anion indicates a failed modification.] The results of the Ellman's reagent test were further confirmed by mass spectroscopy. The modified β-chain mass of 15 987 Da, 120 Da greater than the native β-chain mass, is consistent with the additional mass expected for the *N*-ethylsuccinimido group.

The digestion of Arg α141 to produce the des-Arg modification was performed according to published procedures (*22*). One gram of the NES hemoglobin was gel-filtered against fresh 0.2 M barbitol buffer at pH 8.2 and brought to a concentration of 10 mg/mL. To this, 0.7 mg of type I carboxypeptidase B was added, and the mixture was allowed to react for 3 h at 25 °C. The enzyme was then removed by gel filtration on a 4 × 40 cm Sephadex G-25 fine column, followed immediately by filtration on a 4 × 8 cm DE-52 column, both columns equilibrated with 0.01 M sodium phosphate buffer at pH 6.9. Finally, the sample was dialyzed against 0.05 M Bis-Tris [bis(2-hydroxyethyl)iminotris(hydroxymethyl)methane] buffer with 0.1 M sodium chloride at pH 7.0. Arginine removal was confirmed by mass spectroscopy.

The T-state NES-des-Arg-hemoglobin samples (T_0) were further modified by phosphate stripping at a rate of 15 mL/h at 4 °C on a 2 × 25 cm Sephadex G-25 fine column equilibrated with 0.05 M Bis-Tris buffer with 0.1 M NaCl at pH 7.0. Samples were then dialyzed overnight against 0.05 M Bis-Tris buffer containing 0.1 M NaCl and 10 mM IHP at pH 7.0 (*23*).

The final concentration of NES-des-Arg samples used in the MCD measurements was 280 μM in heme, determined by deoxy absorbance at 558 nm ($\epsilon_{558} = 12.5 \times 10^3$ cm^{-1} M^{-1}). The samples were deoxygenated under a flow of humidified argon by irradiation with a high-intensity, low-heat lamp. Approximately one grain of sodium dithionite was added to the sample to reduce any excess oxygen in solution. UV−vis absorption spectroscopy showed the presence of less than 3% metHb. Ligated samples (R_4) were prepared by placing deoxy samples under a flow of humidified carbon monoxide at about 1 atm for 20 min. Full ligation was confirmed by UV−vis spectroscopy.

Samples of hemoglobin from *Cyprinus carpio* were purified and prepared in the oxygenated form at the University of Nebraska (*24*). Sample concentrations for the CD and MCD spectral measurements were about 220 μM in heme. R-State samples were prepared in 0.05 M borate buffer at pH 9.0, whereas T-state samples were prepared in 0.01 M potassium phosphate with 1 mM IHP at pH 6.0. Deoxy (R_0, T_0) and carboxy samples (R_4, T_4) were prepared as described for human hemoglobin.

Magnetic Circular Dichroism. Magnetic circular dichroism measurements were performed on a commercial circular dichrometer, its sample compartment outfitted with a 0.68 T permanent magnet. Measurements were carried out in a sealed 1-mm path length quartz cuvette. The sample cuvette was mounted in a water-jacketed cell holder interfaced with a water bath maintaining the cuvette temperature at 7 °C. A flow of nitrogen through the sample compartment prevented condensation on the cuvette cell walls and aided in temperature regulation. MCD measurements were made every 0.5 nm over a wavelength range of 240−340 nm, with a bandwidth of 1 nm and a total data accumulation time of 8 s/wavelength. The sample was checked by UV−vis absorption spectroscopy for sample degradation from oxygen contamination. The MCD was determined as the difference of measurements made at opposed field polarities in order to cancel the natural CD of the sample. The data were smoothed by a 15-point Savitzky−Golay polynomial procedure (*25*). All hemoglobin MCD and CD spectra are reported on a per-tetramer basis.

Calculated Tryptophan MCD Contributions. The absolute MCD spectra of all samples were first normalized to concentration on the basis of the absorption of the deoxy form at 558 nm, a procedure with an overall precision of about 10%. Absolute MCD spectra of the tryptophan bands, minus the broader and more intense background signal from the porphyrin L bands of the heme chromophores, were then obtained by applying a spectral subtraction procedure and these were calibrated more precisely to relative concentration, as described below. The subtraction procedure took advantage of the different ratios of heme and tryptophan MCD chromophores found in hemoglobins derived from humans and carp (heme:tryptophan ratios of 4:6 and 4:12, respectively) in order to disentangle the separate contributions of each chromophore to a particular sample. These procedures also assumed that the effects of protein quaternary conformation on the observed MCD spectra were generally small and localized to the tryptophan contributions and that the species differences between heme contributions were negligible.

The MCD spectra of the seven samples studied, human R_4, R_0, and T_0 and carp R_4, R_0, T_4, and T_0, were first modeled as the sum of separate tryptophan and deoxy or carboxy heme contributions, ignoring for the moment any effects of protein quaternary conformation or species differences in primary structure on the component spectra. In matrix form this is

$$\mathrm{MCD} = \mathrm{Components} \cdot \mathrm{Coefficients}$$

where MCD is a matrix containing the observed human (h) and carp (c) spectra as columns

$$\mathrm{MCD} = [\, R_0^{(h)}\ T_0^{(h)}\ R_4^{(h)}\ R_0^{(c)}\ T_0^{(c)}\ R_4^{(c)}\ T_4^{(c)}]$$

the component matrix contains as columns the "zeroth-order"

conformation-independent chromophore spectra to be determined

$$\text{Components} = [\text{deoxyheme}^{(o)} \quad \text{carboxyheme}^{(o)} \quad \text{tryptophan}^{(o)}]$$

and

$$\text{Coefficients} = \begin{bmatrix} 4 & 4 & 0 & 4 & 4 & 0 & 0 \\ 0 & 0 & 4 & 0 & 0 & 4 & 4 \\ 6 & 6 & 6 & 12 & 12 & 12 & 12 \end{bmatrix}$$

contains the chromophore stoichiometries. The least-squares solution for the component spectra is given by

$$\text{Components} = \text{MCD} \cdot \mathit{pinv}(\text{Coefficients})$$

where *pinv* is the matrix pseudoinverse. The application of further smoothing (40-point Savitzky−Golay) to the broad heme component spectra removed a small amount of spurious spectral structure caused by incomplete separation from the much narrower tryptophan bands.

More accurate tryptophan component spectra reflecting protein structural effects were then obtained by subtracting the appropriate deoxy or carboxy heme component found in the previous step from the observed spectra. For example, the expression

$$\text{Trp}(R_0^{(h)}) = [R_0^{(h)} - 4 \cdot \text{deoxyheme}^{(o)}]/6$$

yielded the average tryptophan signal for human R_0. Finally, the tryptophan spectra were normalized more precisely to relative concentration *c*, as determined by comparing the observed spectra to the zeroth-order model spectra. For instance, the concentration factor for the human R_0 spectrum was obtained from the proportionality relation

$$R_0^{(h)} = c(R_0^{(h)})\,[4 \cdot \text{deoxyheme}^{(o)} + 6 \cdot \text{tryptophan}^{(o)}]$$

where the spectra are column vectors. The band shapes of the observed and model spectra, while very similar, are not in general identical. In this case, the *n* equations arising from the proportionality relation, where *n* is the number of wavelength components in the spectral vectors, are linearly independent and *c* is overdetermined. The best value of *c* in a least-squares sense was thus determined by matrix inversion of the previous expression to yield

$$c(R_0^{(h)}) = \mathit{pinv}([4 \cdot \text{deoxyheme}^{(o)} + 6 \cdot \text{tryptophan}^{(o)}]) \cdot R_0^{(h)}$$

The tryptophan spectra normalized in this manner were used to calculate the difference spectra reported below, such as the R − T difference spectrum for human deoxy Hb, $\text{Trp}(R_0^{(h)})/c(R_0^{(h)}) - \text{Trp}(T_0^{(h)})/c(T_0^{(h)})$, for example.

RESULTS

The near-UV CD spectra of unligated NES-des-Arg-hemoglobin in the relaxed and tense states and the $R_0 - T_0$ difference spectrum are shown in Figure 2A. The positive R − T difference with maxima at 278, 282, and 287 nm was attributed by Perutz et al. to changes in the relative orientations of the aromatic amino acids in the R and T states. Similar difference spectra are observed for the carp samples,

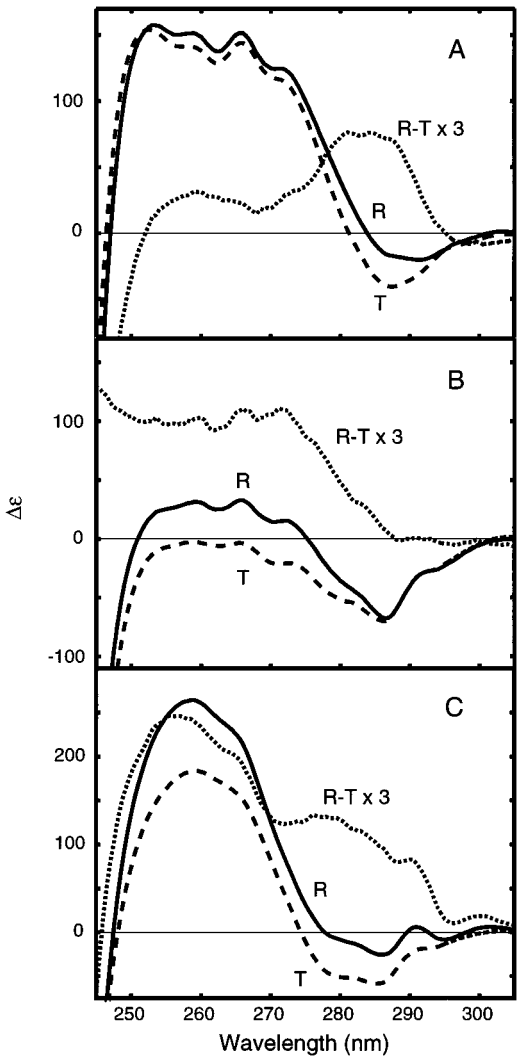

FIGURE 2: Near-UV CD spectra of R (—) and T (- - -) states and R − T differences (···): (A) deoxy NES-des-Arg human hemoglobin; (B) deoxy carp hemoglobin; (C) carbonmonoxy carp hemoglobin. The difference spectra are multiplied by 3.

although the magnitude is much diminished, and the band is broader and blue-shifted by about 15 nm, in the unliganded carp hemoglobin (Figure 2B) relative to liganded (Figure 2C).

The near-UV MCD spectra of all seven hemoglobin samples studied, the R_0, T_0, and R_4 forms of NES-des-Arg human hemoglobin and the R_0, T_0, R_4, and T_4 forms of carp hemoglobin, are shown in Figure 3. The largest differences between these spectra arise from the heme contributions, which depend very strongly on ligation state. This is in contrast to the similarity between absorption spectra (*2*) for the carboxy and deoxy forms. In examining the MCD for a given ligation state, little difference in band shape is observed between the human and carp hemoglobin samples. Accordingly, the heme MCD contributions to the spectra in Figure 3 were isolated by exploiting the different ratios of heme and tryptophan chromophores present in human and carp hemoglobins, as described above. The heme component spectra are shown in Figure 4. The deoxyheme spectrum has negative extrema near 260 and 323 nm and a positive extremum near 293 nm, whereas the carboxy spectrum has positive extrema near 266 and 315 nm and a broad negative extremum centered about 290 nm. This is to our knowledge

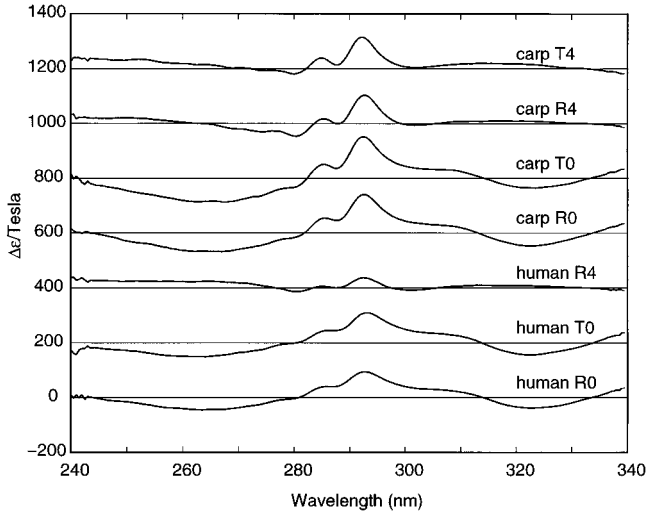

FIGURE 3: Near-UV MCD spectra of R_0, T_0, and R_4 states of NES-des-Arg human hemoglobin and R_0, T_0, R_4, and T_4 states of carp hemoglobin. Liganded samples are complexed with CO. Spectra are displayed in listed order offset by increasing increments of 200 on the vertical axis from that of human R_0.

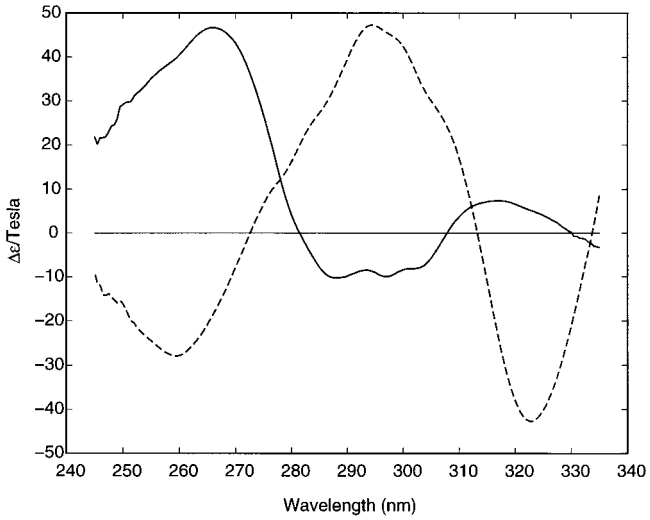

FIGURE 4: Near-UV MCD spectra of carbonmonoxy (—) and deoxy (- - -) heme components calculated from human and carp hemoglobin spectra in Figure 3. See Experimental Procedures for component spectra calculations.

the first MCD study of the aromatic region of a heme protein, but the UV MCD spectra of some protoporphyrin derivatives have been reported by Shimizu et al. (*27*). In particular, the UV MCD spectrum of carboxyheme in hemoglobin shown in Figure 4 is roughly similar to that of the low-spin CO complex of ferrous protoporphyrin IX observed in 50% aqueous ethanol solution, the latter complex apparently serving as an approximate model compound for the protein chromophore despite the replacement of the histidinyl ligand present in the protein with a solvent molecule as the fifth ligand. Shimizu et al. suggest that the short-wavelength pair of MCD extrema observed in the complex may possibly be assigned to an A term arising from the porphyrin L or N bands. The corresponding extrema in the carboxyheme spectrum are centered nearest the L absorption band.

The tryptophan MCD bands comprise a peak of positive ellipticity at 292 nm that is assigned to the vibronic origin of the ^1L_b electronic transition (Platt notation), a smaller peak at 284 nm assigned to the 0−730 vibronic band of the ^1L_b transition, and a broad trough at 268 nm, the ^1L_a band, all bands being assigned to B terms (*4*). The two lowest energy tryptophan bands are easily distinguished from the broader heme bands that overlap them. The differences observed between the tryptophan bands in the various hemoglobin samples are small, with the exception of the doubling in intensity of the carp tryptophan bands relative to those of human hemoglobin that is expected from the chromophore stoichiometries. This is consistent with the noted application of MCD as a method for quantitatively determining tryptophan content, at least in nonallosteric and non-heme proteins (*4*).

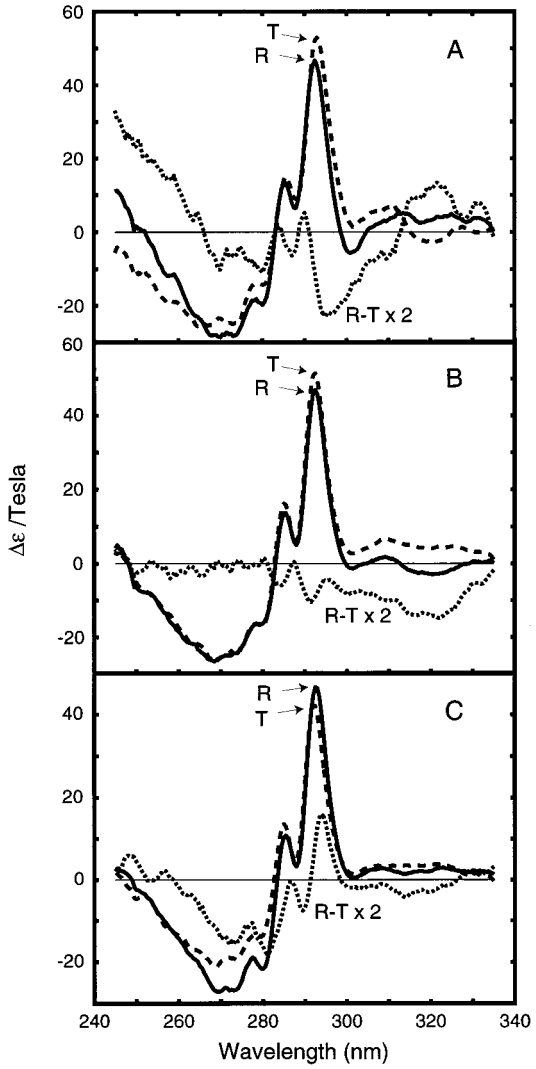

FIGURE 5: Tryptophan component spectra calculated from the MCD spectra in Figure 3 for R (—) and T (- - -) states and R − T differences (•••): (A) deoxy NES-des-Arg human hemoglobin; (B) deoxy carp hemoglobin; (C) carbonmonoxy carp hemoglobin. The difference spectra are multiplied by 2. See Experimental Procedures for component spectra calculations.

The dependence of tryptophan band shape and position on protein quaternary conformation is brought out more clearly in the tryptophan component and R − T difference MCD spectra shown in Figure 5. The human $R_0 - T_0$ difference (Figure 5A) has a peak-to-trough magnitude that is about 30% of the R-state maximum. This difference arises mainly from the 0.5 nm blue shift and 14% increase in intensity of the 293-nm peak in the T state relative to R. The $R_0 - T_0$ difference spectrum observed in carp (Figure

5B) is much smaller, reflecting the near lack of band shift or intensity difference between R and T states. The $R_4 - T_4$ difference spectrum (Figure 5C), observed only in carp, is roughly the reverse of the $R_0 - T_0$ difference observed in human hemoglobin, reflecting the 0.6 nm red shift and 10% decrease in intensity of the 293-nm peak in the T state relative to R.

DISCUSSION

Perutz et al. (*2*) previously assigned the features in the near-UV R − T absorption difference spectrum of NES-des-Arg-hemoglobin to changes in the Trp β37 absorption and possibly to changes in Tyr α42 absorption as well. These spectral features can now be assigned more specifically by use of the combined information from CD and MCD measurements, which provides more differential sensitivity to these aromatic amino acids. The positions of three of the five features observed in the near-UV absorption signal are retained in the CD difference spectrum shown in Figure 2, specifically those occurring at 278, 282, and 287 nm. Only two peaks appear in the MCD difference spectrum (Figure 5), those at 287 and 292 nm. A comparison of MCD band sign and location in Figure 5 with the solution spectrum of L-tryptophan ethyl ester hydrochloride and the tryptophan peaks at 287 and 293 nm observed in lysozyme (*4*) identifies these peaks in the NES-des-Arg spectrum as characteristic of tryptophan. Although Perutz et al. suggested that the 287-nm feature in the absorption difference spectrum may be due to Tyr α42, it is now clear from its presence in the CD and MCD spectra that this peak is most probably associated with a tryptophan residue(s), presumably Trp β37. An assignment to Tyr α42 is ruled out principally because tyrosine can contribute only a negative MCD signal (*4*), in disagreement with the positive MCD sign observed for the 287-nm peak in the absolute spectrum. Moreover, the MCD intensity of a tyrosine residue is expected to be about an order of magnitude weaker than that of a tryptophan. Similarly, the extinction coefficient of tryptophan ($\epsilon \sim 5000$ cm^{-1} M^{-1}) is much greater than that of tyrosine ($\epsilon \sim 1400$ cm^{-1} M^{-1}), so that small tyrosine contributions will generally be buried under much stronger tryptophan signals in this spectral region (*28*). The assignments of the other peaks in the absorption difference spectrum by Perutz et al. are retained. The small peak at 302 nm assigned to tryptophan apparently corresponds to a transition with very low MCD activity. The 278 nm peak present in the CD difference spectrum does not appear in the MCD difference spectrum and is therefore reasonably assigned on the basis of its spectral location to a tyrosine band.

X-ray diffraction studies of human deoxyhemoglobin show that Trp β37 is hydrogen-bonded to the negatively charged carboxylate group of the Asp α94 side chain in the T state, an interaction that is missing in the R state (*13*). Evidence for this hydrogen bond in the solution state of HbA is provided by UV resonance Raman (*29*) and NMR (*30*−*32*) studies. A change in hydrogen-bonding status is expected to provide a dominant perturbation to the electronic spectrum of Trp β37 and is consistent with the shift of the absorption of the proton-donating indole side chain to longer wavelengths observed here upon the transformation of NES-des-Arg-hemoglobin from the R state to the T state by addition of IHP. (Buffer effects were ruled out by control experiments measuring spectra for the R and T conformations under identical buffer and pH conditions. Although IHP was present in solution for the T-state measurements, but not the R, IHP has not been observed to directly affect the absorption spectra of aromatic residues.) If we assume that all of the observed wavelength shift arises from the two Trp β37 residues present in human Hb, then we can estimate that the energy of the L_b transition for each Trp β37 in the tetramer is shifted by about 200 cm^{-1}. The magnitude of this red shift is in good agreement with that expected for a hydrogen-bond proton donor (*33*).

The R → T modulation in Trp β37 MCD intensity observed in the modified human hemoglobin sample may also be explained as a correlate of hydrogen bonding. In the Michl perimeter model of aromatic MCD, the sign of the lowest energy electronic transition is determined mainly by the double energy difference, ΔHOMO − ΔLUMO, between the four frontier orbitals (*6*). In particular, if ΔHOMO, the magnitude of the energy difference between the highest occupied molecular orbitals, is smaller than ΔLUMO, the corresponding magnitude for the lowest unoccupied molecular orbitals, then the sign of the MCD ellipticity of the lowest energy band will be positive. Souto et al. (*34*) explained the MCD sign of tryptophan in the context of the perimeter model by considering it as a derivative of the indenide anion, the latter being a "soft" MCD chromophore in the sense that ΔHOMO ≈ ΔLUMO. Formally replacing a -CH-$^-$ moiety in the anion with the more electron-donating -NH- moiety to form indole causes ΔHOMO to become smaller than ΔLUMO (ΔHOMO − ΔLUMO = −0.13 eV). The intensity of the resulting positive ellipticity is expected in this model to be further increased by donation of a hydrogen-bond proton from the indole ring to aspartate, as observed, because proton donation increases the electron-donating character of the indole nitrogen.

The MCD band shift and intensity change observed for tryptophan in NES-des-Arg human hemoglobin are directly correlated in the perimeter model with the change in hydrogen-bonding status of the Trp β37 at the $\alpha_1\beta_2$ interface expected during the quaternary structure change induced by IHP. The contrasting R − T differences observed in the deoxy and carboxy carp hemoglobins thus raise the question of whether they reflect differences in the quaternary structure change or result from the different pH conditions and tryptophan constituents for the carp and human hemoglobins. Crystal structures for carp hemoglobin are not available, but the α- and β-chain sequence homologies and functional similarities between carp and human hemoglobins are relatively high. In particular, the Trp β37 and its interacting residues at the $\alpha_1\beta_2$ interface, Asp α94, Arg α92, Arg α141, and Pro α95, present in human hemoglobin are conserved in carp hemoglobin. It thus seems very likely that the effect of the quaternary structure change on the Trp-β37 MCD spectrum deduced for human hemoglobin is also present in carp. This conclusion is strengthened by the similarities observed between carp and human hemoglobins in both the aromatic-region R − T CD difference spectra (Figure 2) and the R − T intensity differences in intrinsic aromatic fluorescence (*35*). The divergences observed between the tryptophan MCD R − T spectra of human and carp hemoglobins in Figure 5 are thus more likely due to some additional effect present in the carp but not the human

hemoglobin measurements rather than a different effect of quaternary structure on Trp β37. One such factor is the use of the Root effect to manipulate quaternary state in carp hemoglobin, a procedure that necessarily involves large changes in pH (3 pH units in the present study), as opposed to the constant pH conditions used in the human hemoglobin measurements. Although this pH change is not expected to affect the Trp β37−Asp α94 H-bond interaction at the dimer−dimer interface, the pK_as of tryptophan and aspartic acid both lying outside the range in question, the protonation of imidazolic nitrogen could affect any tryptophan−histidine interactions that might be present. The general molecular mechanism of the Root effect in fish hemoglobins remains controversial (*36*−*39*), but about half of the effect comes from the β-chain carboxy-terminal histidine (His β147) also responsible for the chloride-independent Bohr effect in human hemoglobin. The crystal structure of a Root effect hemoglobin from the teleost fish *Leiostomus xanthurus* (*38*) suggests that in carp hemoglobin this histidine may be too far removed from the nearest tryptophan, Trp β3, to perturb the latter's spectrum upon imidazole protonation. However, an adjacent histidine−tryptophan pair, His α45 and Trp α46, does occur in the sequence of the carp α chains (but not in HbA). Moreover, the formation of a His α45−Trp α46 charge transfer complex has been suggested previously as an explanation for the drop in aromatic fluorescence intensity observed in carbonmonoxy carp hemoglobin at acidic pH (in the absence of IHP) (*35*). Positive charge donation from histidine to tryptophan would be expected to blue-shift the (low-pH) T-state absorption band of Trp α46 relative to the (high-pH) R state and reduce the T-state MCD intensity in the perimeter model, as observed in liganded carp hemoglobin. The band shift and MCD intensity changes observed in the carp samples can thus be understood as a summing of oppositely signed spectral changes for at least two of the six types of tryptophans present in the protein, Trp β37 and Trp α46. Their effects apparently cancel one another for the unliganded sample, whereas the T-state blue shift posited for Trp α46 appears to dominate in liganded carp Hb. The origin of the ligation-dependent difference within the carp R − T spectra is not clear, however. In this regard, the possible contributions of pH-dependent interactions involving other tryptophans (Trp β131 in carp; Trp α14 and β15 in both human and carp) are difficult to assess.

Recent crystallographic evidence for a second R-like quaternary structure in human hemoglobin, designated Y (*40*) or R2 (*41*), has raised the question as to which structure, R2/Y or the canonical R structure, is most representative of liganded hemoglobin under physiological conditions (*42*, *43*). The steric barrier presented by movement of the imidazole side chain of His $\beta_2$97 past the Thr $\alpha_1$41 residue is thought to provide an important component of the energetic barrier between the R and T states. The His $\beta_2$97 side chain is positioned between Pro $\alpha_1$44 and Thr $\alpha_1$41 in the T state and between Thr $\alpha_1$41 and Thr $\alpha_1$38 in the canonical R structure but is rotated out of the latter pocket in the R2 structure (*41*). Despite this difference in structure at the switch region of the $\alpha_1\beta_2$ interface, however, the R2 and R structures are very similar with regard to hydrogen bonding and contact interactions in the flexible joint region. Thus, the spectral results in the present work regarding Trp β37 and its hydrogen-bonding interactions in the joint region are not expected to shed further light on the issue of the R versus the R2 quaternary structures.

In conclusion, we report near-UV CD and MCD spectra for carp and NES-des-Arg modified human hemoglobins demonstrating that structural change associated with the R → T quaternary transition can be detected in human hemoglobin by measuring the MCD of the aromatic amino acids. In contrast to the correspondence with global quaternary structure changes observed previously for the near-UV natural CD, the magnetic CD changes observed in the present work can be assigned to a specific dimer−dimer interaction. Our MCD results strongly suggest that the blue-shifting and intensity increase of the tryptophan L_b band are correlated with the formation of a hydrogen bond between Asp $\alpha_1$94 and Trp $\beta_2$37 in the $\alpha_1\beta_2$ joint region as the protein moves from the R to the T state. The observation of this correlation appears to be obscured in carp hemoglobin, on the other hand, by the presence of additional tryptophans β3, α46, and β131, at least one of which, α46, is acid-labile due to the presence nearby of an imidazolic nitrogen from a histidine residue.

The direct correlation observed in the present work between the near-UV MCD and the quaternary state of human hemoglobin allows changes in tryptophan MCD band position and intensity to be used as monitors of allosteric dynamics in the $\alpha_1\beta_2$ region of the protein in time-resolved MCD experiments. Along these lines, the results of preliminary time-resolved near-UV MCD experiments on photolyzed carbonmonoxy HbA appear to provide further evidence for an early microsecond change in the Trp β37 environment at the dimer−dimer interface preceding the 20-μs process conventionally assigned to the R → T transition (R. M. Esquerra, R. A. Goldbeck, and D. S. Kliger, unpublished results).

REFERENCES

1. Perutz, M. F. (1970) *Nature 228*, 726−739.
2. Perutz, M. F., Ladner, J. E., Simon, S. R., and Ho, C. (1974) *Biochemistry 13*, 2163−2173.
3. Björling, S. C., Goldbeck, R. A., Paquette, S. J., Milder, S. J., and Kliger, D. S. (1996) *Biochemistry 35*, 8619−8627.
4. Barth, G., Voelter, W., Bunnenberg, E., and Djerassi, C. (1972) *J. Am. Chem. Soc. 94*, 1293−1298.
5. McFarland, T. M., and Coleman, J. E. (1972) *Eur. J. Biochem. 29*, 521−527.
6. Michl, J. (1978) *J. Am. Chem. Soc. 100*, 6801−6811 and 6812−6824.
7. Hirsch, R. E., and Nagel, R. L. (1981) *J. Biol. Chem. 256*, 1080−3.
8. Itoh, M., Mizukoshi, H., Fuke, K., Matsukawa, S, Mawatari, K., Yoneyame, Y., Sumitani, M., and Yoshihara, K. (1981) *Biochem. Biophys. Res. Commun. 100*, 1259−1265.
9. Hirsch, R. E. (1994) *Methods Enzymol. 232*, 231−246.
10. Sutherland, J. C., and Low, H. (1976) *Proc. Natl. Acad. Sci. U.S.A. 73*, 276−280.
11. Hicks, B., White, M., Ghiron, C. A., Kuntz, R. R., and Volkert, W. A. (1978) *Proc. Natl. Acad. Sci. U.S.A. 75*, 1172−1175.
12. Wetlaufer, D. B. (1962) *Adv. Protein Chem. 17*, 303−390.
13. Vallone, B., Bellelli, A., Miel, A. E., Brunori, M., and Fermi, G. (1996) *J. Biol. Chem.* 271, 12472−12480.
14. Benesch, R. E., and Benesch, R. (1962) *Biochemistry 1*, 735−738.
15. Guidoti, G., and Konigsberg, W. (1964) *J. Biol. Chem. 239*, 1474−1484.
16. Kilmartin, J. V., and Hewitt, J. A. (1972) *Cold Spring Harbor Symp. Quant. Biol. 36*, 311−314.
17. Perutz, M. F., Muirhead. H., Mazzarella, L., Crowther, R. A., Greer, J., and Kilmartin, J. V. (1969) *Nature 222*, 1240−1243.

18. Riggs, A. (1961) *J. Biol. Chem. 236*, 1948−1954.
19. Kavanaugh, J. S., Chafin, D. R., Arnone, A., Mozzarelli, A., Rivetti, C., Rossi, G. L., Kwiatkowski, L. D., and Noble, R. W. (1995) *J. Mol. Biol. 248*, 136−150.
20. Geraci, G., Parkhurst, L. J., and Gibson, Q. H. (1969) *J. Biol. Chem. 244*, 4664−4667.
21. Savas, M. M., Shaw, C. F., III, and Petering, D. H. (1993) *J. Inorg. Biochem. 52*, 235−249.
22. Kilmartin, J. V. (1981) *Methods Enzymol. 76*, 167−171.
23. Berman, M., Benesch, R., and Benesch, R. E. (1971) *Arch. Biochem. Biophys. 145*, 236−239.
24. Goss, D. J., and Parkhurst, L. J. (1984) *Biochemistry 23*, 2174−2179.
25. Savitzky, A., and Golay, M. J. E. (1964) *Anal. Chem. 36*, 1627−1639.
26. Briehl, R. W., and Hobbs, J. F. (1970) *J. Biol. Chem. 245*, 544−554.
27. Shimizu, T., Nozawa, T., and Hatano, M. (1976) *Bioinorg. Chem. 6*, 77−82.
28. Cantor, C. R., and Schimmel, P. R. (1980) *Biophysical Chemistry, Part II: Techniques for the Study of Biological Structure and Function*, Freeman, New York.
29. Nagai, M., Kaminaka, S., Ohba, Y., Nagai, Y., Mizutani, Y., and Kitagawa, T. (1995) *J. Biol. Chem. 270*, 1636−1642.
30. Fung, L. W.-M., and Ho, C. (1975) *Biochemistry 14*, 2526−2535.
31. Asakura, T., Adachi, K., Wiley, M. S., Fung, L. W.-M., Ho, C., Kilmartin, J. V., and Perutz, M. F. (1976) *J. Mol. Biol. 104*, 185−195.
32. Ishimori, K., Imai, K., Miyazaki, G., Kitagawa, T., Wada, Y., Morimoto, H., and Morishima, I. (1992) *Biochemistry 31*, 3256−3264.
33. Pimentel, G. C., and McClellan, A. L. (1960) *The Hydrogen Bond*, Freeman, San Francisco, CA.
34. Souto, M. A., Wallace, S. L., and Michl, J. (1980) *Tetrahedron 36*, 1521−1530.
35. Hirsch, R. E., and Noble, R. W. (1987) *Biochim. Biophys. Acta 914*, 213-219.
36. Ito, N., Komiyama, N. H., and Fermi, G. (1995) *J. Mol. Biol. 250*, 648−658.
37. Perutz, M. F. (1996) *Nat. Struct. Biol. 3*, 211−212.
38. Mylvaganam, S. E., Bonaventura, C., Bonaventura, J., and Getzoff, E. D. (1996) *Nat. Struct. Biol. 3*, 275−283.
39. Mazzarella, L., D'Avino, R., di Prisco, G., Savino, C., Vitagliano, L., Moody, P. C. E., and Zagari, A. (1999) *J. Mol. Biol. 287*, 897−906.
40. Smith, F. R., Lattman, E. E., and Carter, C. W. (1991) *Proteins: Struct., Funct., Genet. 10*, 81−91.
41. Silva, M. M., Rogers, P. H., and Arnone, A. (1992) *J. Biol. Chem. 267*, 17248−17256.
42. Srinivasan, R., and Rose, G. D. (1994) *Proc. Natl. Acad. Sci. U.S.A. 91*, 11113−11117.
43. Schumacher, M. A., Zheleznova, E. E., Poundstone, K. S., Kluger, R., Jones, R. T., and Brennan, R. G. (1997) *Proc. Natl. Acad. Sci. U.S.A. 94*, 7841−7844.

BI992823A